Electronic Supplementary Information (ESI)

Cathodic Corrosion Activated Fe-based Nanoglass as Highly-Active and -Stable Oxygen Evolution Catalyst for Water Splitting

Kaiyao Wu[a], Fei Chu[a], Yuying Meng[a], Kaveh Edalati[b], Qingsheng Gao[c], Wei Li[a], Huai-Jun Lin[a, *]

[a] Institute of Advanced Wear & Corrosion Resistance and Functional Materials, Jinan University, Guangzhou 510632, PR China

[b] International Institute for Carbon-Neutral Energy Research (WPI-I2CNER), Kyushu University, Fukuoka 819-0395, Japan

[c] Department of Chemistry, Jinan University, Guangzhou, 510632, China

* Corresponding author, Email: hjlin@jnu.edu.cn

Experimental section

Materials Preparation

The reasons why we choose $Fe_{78}Si_9B_{13}$ amorphous alloy as the most research object are as follows: Firstly, the $Fe_{78}Si_9B_{13}$ amorphous alloy is one of the amorphous alloys with the highest proportion of iron (78% of iron), so it is very suitable for application in catalytic reactions that require a large amount of Fe sources, such as OER procless. Secondly, $Fe_{78}Si_9B_{13}$ amorphous alloy have been successfully produced and applied in industrial scale as a classic magnetic materia[1]. Therefore, compared with other amorphous alloys that are still in the experimental synthesis stage, its large-scale use in the field of catalysis has a huge advantage. Moreover, Fe, Si and B are all rich elements in the earth's crust, which shows that $Fe_{78}Si_9B_{13}$ amorphous alloy has low cost and easy access. Finally, $Fe_{78}Si_9B_{13}$ amorphous alloy has excellent catalytic degradation [2] and HER catalytic performance.

The $Fe_{78}Si_9B_{13}$ amorphous alloy ribbons were prepared by melt spinning in a high-purity argon (99.999%) atmosphere (Melt-spun glass, abbreviated as MSG). The ribbons were punched into disc in diameter of 10 mm. Afterwards, about 40-50 discs were overlapped (about 1 mm in thickness) and subjected to the HPT processing at ambient temperature. As a result, $Fe_{78}Si_9B_{13}$ nanoglass (Abbreviated as NG) can be obtain. The HPT parameters were as follows: pressure of 6 GPa, rotation speed of 1 rpm, rotations of 10 turns. Preparation process of materials is illustrated in Fig. S1.

The electrochemical corrosion for the NG and MSG samples are conducted via a typical three-electrode system of a CHI 600E electrochemical workstation (CH,

Instruments, Ins) in 1.0 M KOH at room temperature. To prevent corrosion products (FeOOH) from participating in the reaction (OOH* → O_2) at the high potential of anode [3], the synthesis was processed by cyclic voltammetry (CV) at the cathode with potential window from -1.8 to -1.0 V (vs a saturated Ag/AgCl electrode, RHE) and a scan rate of 100 mV s^{-1}. The NG/MSG samples are served as the working electrode, with an Ag/AgCl as the reference electrode and the carbon rod as the counter electrode. Both NG and MSG samples were executed by 1000 CV, which were denoted as FeOOH@NG and FeOOH@MSG, respectively.

Characterizations.

X-ray diffraction (XRD) experiments were performed on a UItima IV diffractometer (Cu Kα). Field emission scanning electron microscopy (FESEM) measurements were conducted on a TESCAN GAIA3 microscope. Energy dispersive X-ray spectroscopy (EDS) was conducted over a representative area of corroded samples. X-ray photoelectron spectroscopy (XPS) spectra were undertaken on a Thermo Scientific™ K-Alpha™ spectrometer utilizing Al as the photo source. Transmission electron microscopy (TEM) images were obtained by Talos F200S microscope after making the thin foils using focused ion beam (FIB) technique. Differential scanning calorimetry (DSC) was studied the crystallization behavior of materials on a METTLER 3^{+} thermal analyzer. The metal elemental analysis via Inductively coupled plasma-optical emission spectroscopy (ICP-OES) for samples was performed on thermo iCAP 7400 SERIES. Raman spectra were collected on LabRAm HR Evolution with a solid emitter (532 nm) as the exciting source.

Electrochemical Measurements.

The electrochemical measurements were carried out in 1.0 M KOH electrolyte on CHI600E electrochemical workstation with a three-electrode system at room temperature including the Fe-based alloys as the working electrode, a saturated Ag/AgCl as the reference electrode, and a carbon rod as the counter electrode. The CV measurements were carried out for 40 segments to reach a steady state at the scan rate of 100 mV s^{-1} in 1.0 M KOH. Linear sweep voltammetry (LSV) was undertaken with a scan rate of 5 mV s^{-1} for polarization curves (iR compensation 90%). The Tafel plots were obtained from the LSV curve of 5 mV s^{-1} using the Tafel formula ($\eta = a+blogj$) where η, j and b are the overpotential, current density and Tafel slope, respectively. Electrochemical impedance spectroscopy (EIS) measurements were carried out at the potential (vs RHE) at 10 mA cm^{-2} with an amplitude AC voltage of 10 mV and a frequency range from 100 kHz to 0.1 Hz. The double-layer capacitances (C_{dl}) were measured by CV at various scan rates of 30, 60, 90, 120, and 150 mV s^{-1} from 0.08 to 0.18 V (vs RHE). Stability tests were conducted through chronoamperometry at the potential (vs RHE) at 10 mA cm^2 for 48 h. In 1.0 M KOH electrolyte, the potential conversions among E(Ag/AgCl), E(RHE), and η (overpotential) were calibrated in the Fig S2. and the final equations were as follows: E(RHE) =E(vs Ag/AgCl) + 0.197 V + (0.0592 V)pH = E(Ag/AgCl) + 1.020 V, η =E(RHE) − 1.23 V.

Table S1 OER catalytic activities of all samples

B	η（mV）at 10 mA/cm^2	η（mV）at 10 mA/cm^2 After 48h	Onset potential (V)	Tafel slope (mV/dec)	$j_0 \times 10^{-4}$（A/cm^2）	R_{ct} (ohm cm^2)	C_{dl} (mF/cm^2)	ECSA
MSG	436	NA	1.56	88	5.5	2.63	0.73	18
NG	329	350	1.48	76	5.2	7.82	81.40	2035
FeOOH@MSG	347	NA	1.51	61	6.3	20.19	2.33	58
FeOOH@NG	240	278	1.42	42	6.6	55.75	97.50	2438

Table S2 ICP-OES data of MSG and NG samples after electrochemical corrosion and 48h stability test (the iron content in alkaline medium (1 M KOH : 200 ug/L) has been deducted) .

sample	Fe concentration (ug/L)
MSG-48h	1480
FeOOH@MSG-48h	1280
MSG-EC	220
NG-48h	400
FeOOH@NG-48h	240
NG-EC	140

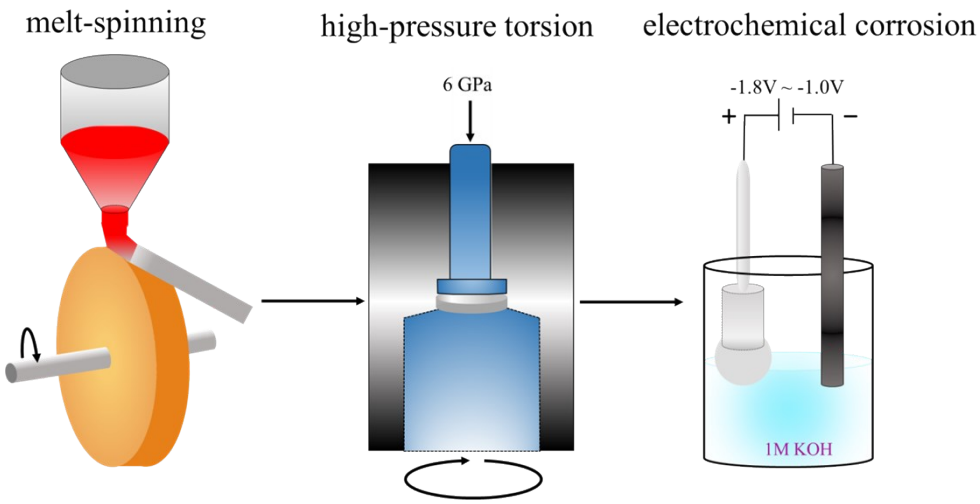

Fig. S1 Preparation process of materials

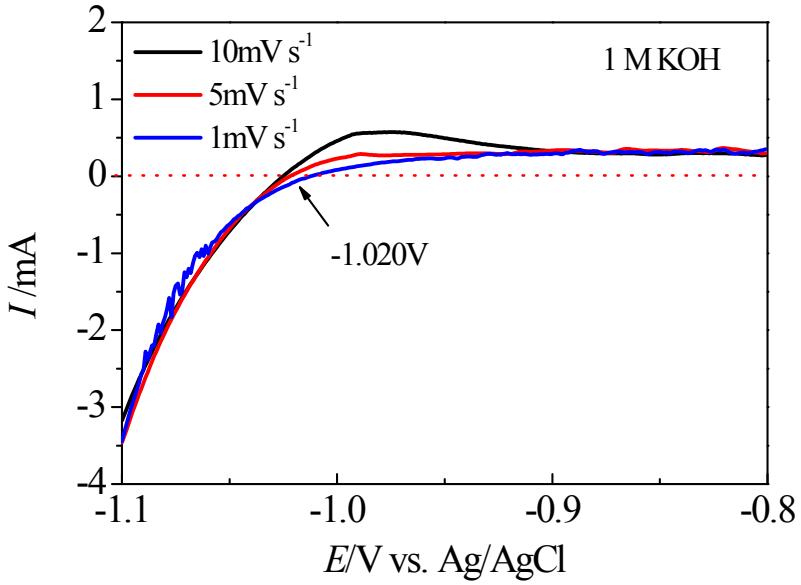

Fig. S2 Polarization curve for calibrating saturated Ag/AgCl reference electrode.

The saturated Ag/AgCl reference electrode calibration

The calibration of saturated Ag/AgCl reference electrode is conducted in a three-electrode setup, including Pt foils as working and counter electrodes with the saturated Ag/AgCl as reference electrode. The 1.0 M KOH electrolyte is saturated with high purity H_2. Linear scanning voltammetry (LSV) is performed at a scan rate of 10 mV s^{-1}, 5 mV $s^{-1}$and 1 mV s^{-1} respectively. The potential window involves the zero current point which can be considered as thermodynamic potential (vs. RHE) for the hydrogen electrode reactions. As shown in Figure S1, the average zero current point is at -1.020 V, thus E (RHE) = E (Ag/AgCl) + 1.020 V.

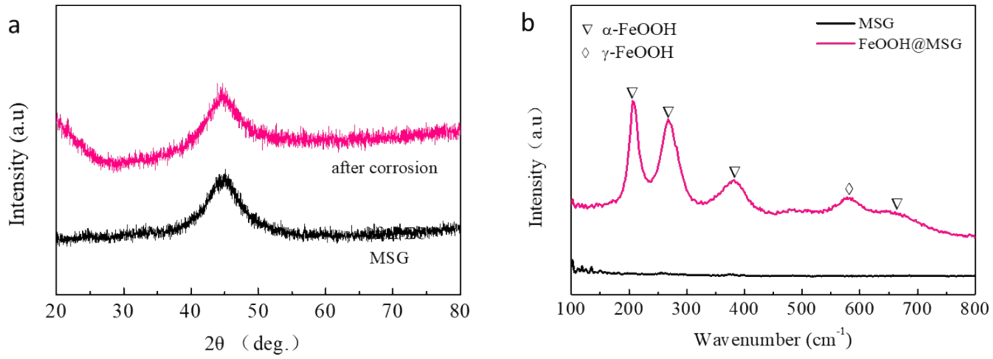

Fig. S3 a) XRD patterns and b) Raman spectroscopy of the MSG sample before and after corrosion

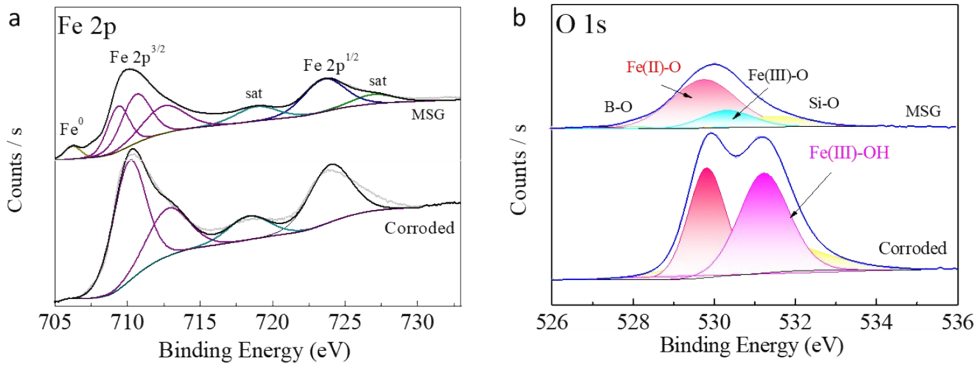

Fig. S4 XPS curves of the MSG sample before and after corrosion : a) Fe 2p, b) O 1s.

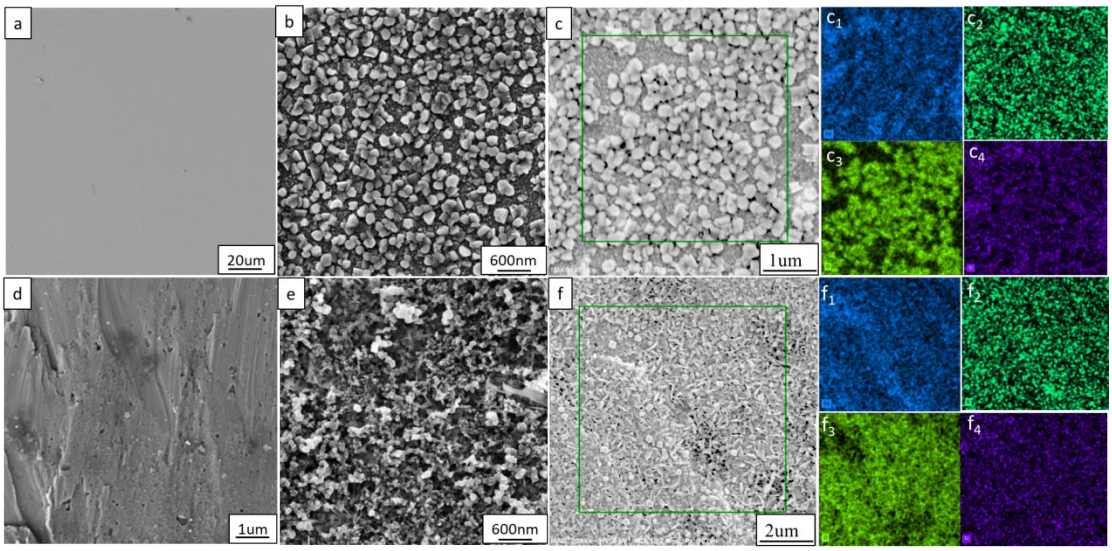

Fig. S5 a-b) FESEM images of the MSG sample before and after corrosion; c) EDS mapping of the FeOOH@MSG sample, c_1-c_4 are Fe, Si, O and B element, respectively; d-e) FESEM images of the NG sample before and after corrosion; f) EDS mapping of the FeOOH@NG sample, f_1-f_4 are Fe, Si, O and B element, respectively.

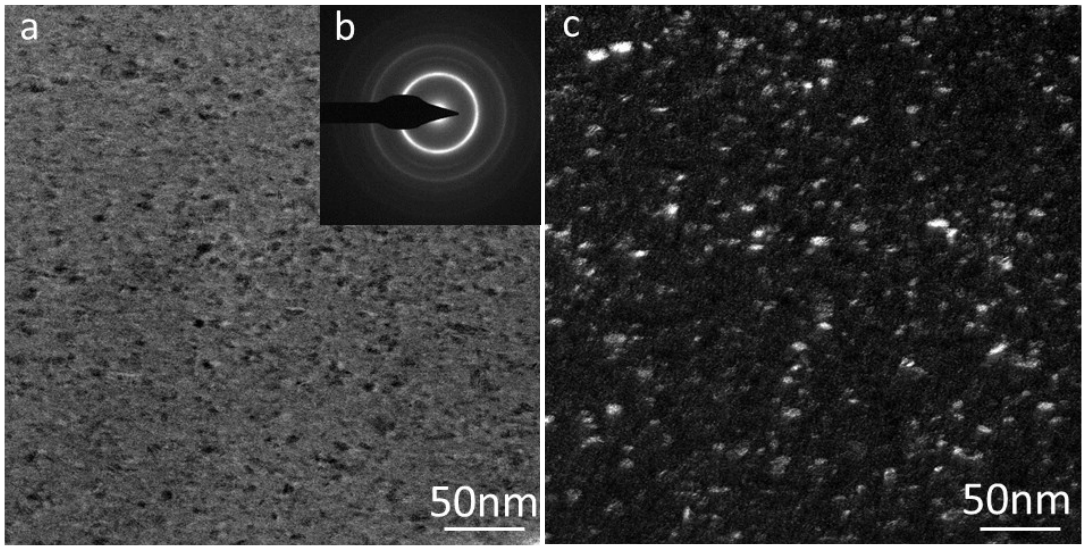

Fig. S6 a) bright-filed TEM image, b) selected area diffraction pattern, c) dark-field TEM image of the Fe_2B phase.

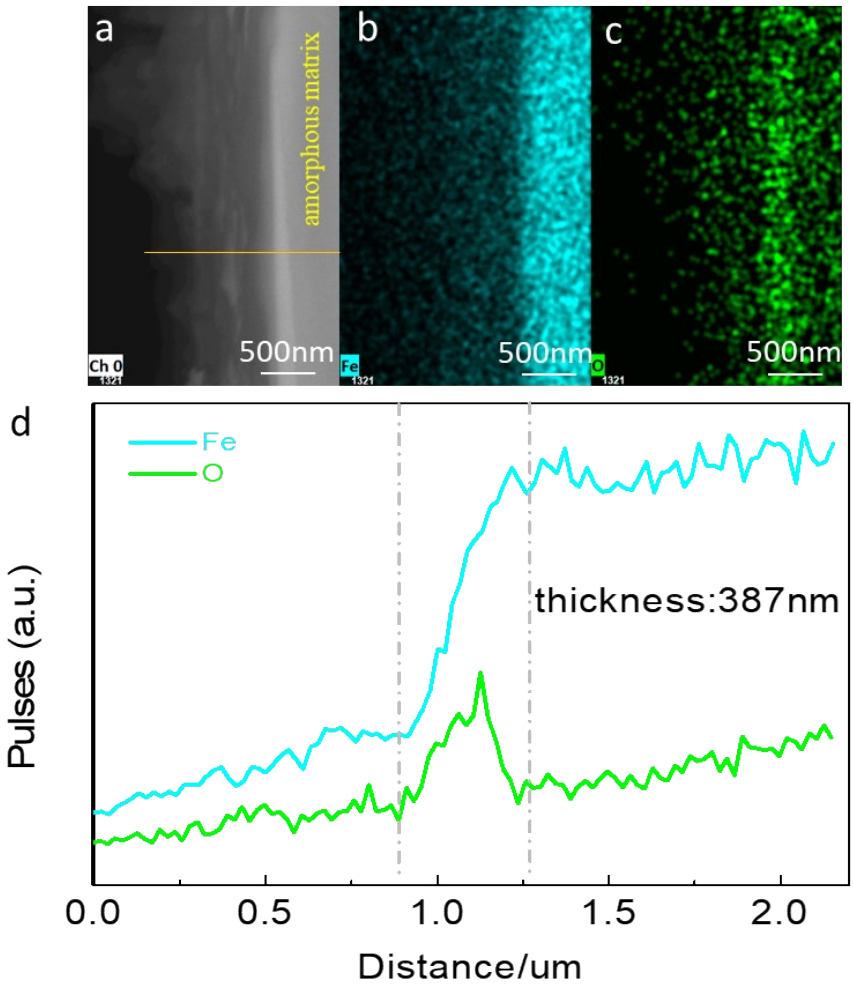

Fig. S7 a-d) EDS mapping and linescan of the cross-section of FeOOH@MSG samples for Fe(f) and O(g).

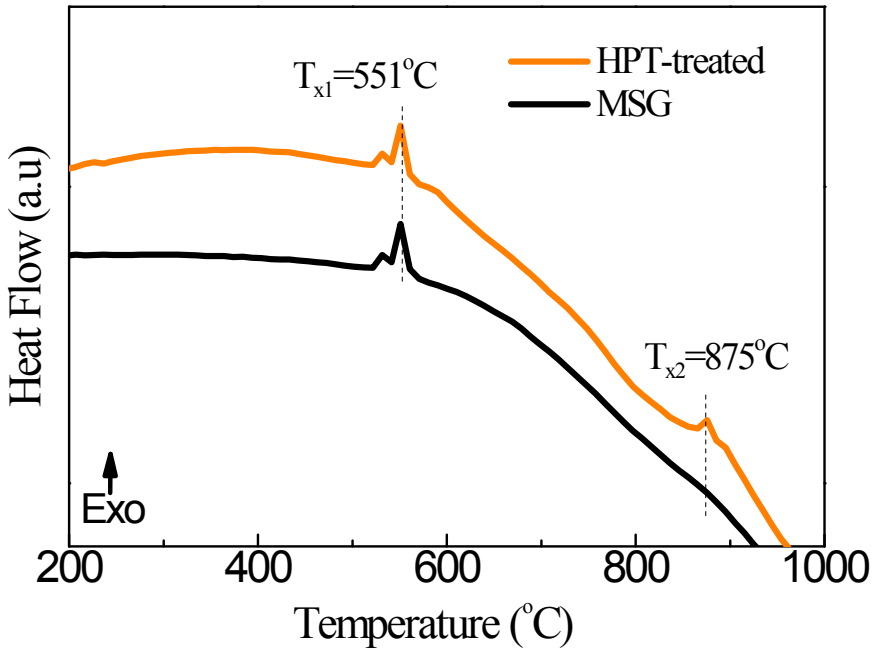

Fig. S8 DSC curves of the $Fe_{78}Si_9B_{13}$ amorphous alloy before and after HPT treatment.

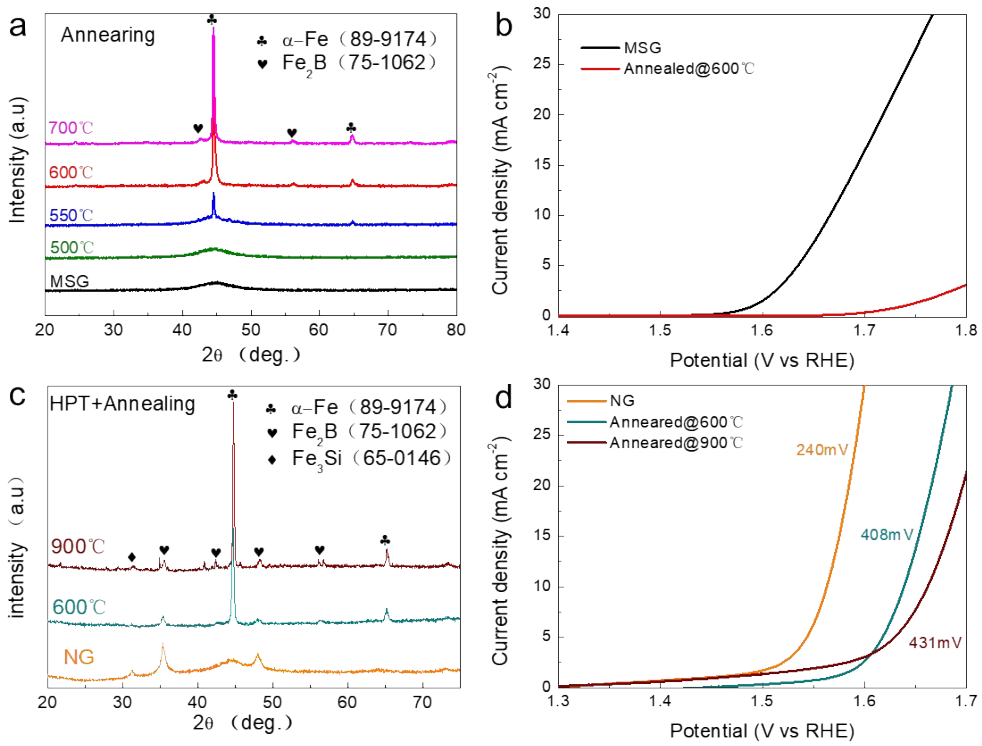

Fig. S9 a) XRD patterns and n) LSV curves of the mlet -spun $Fe_{78}Si_9B_{13}$ amorphous alloy and upon annealing. c) XRD patterns and d) LSV curves of the NG sample and subsequent annealing.

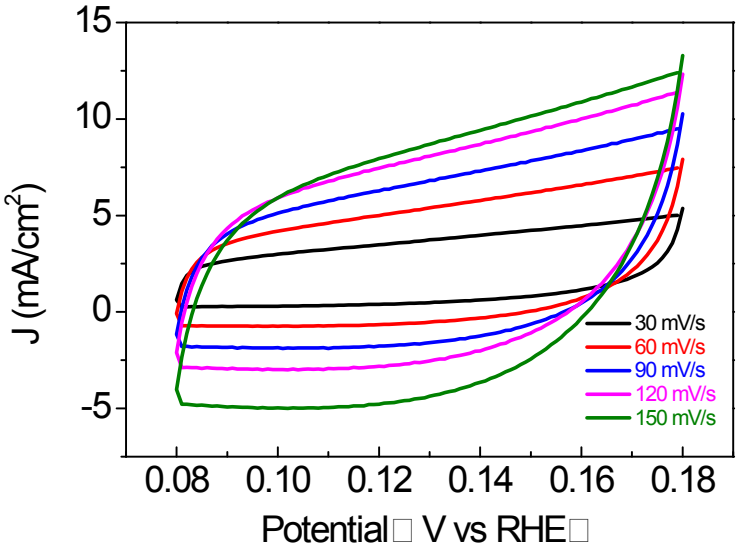

Fig. S10 Measure double-layer capacitance (C_{dl}) with CV curves of different scanning speeds.

Calculation method of electrochemically active surface area (ECSA)

The calculation of ECSA are based on the following equation:

$$ECSA = C_{dl}/C_s$$

C_{dl} is the measured double layer capacitance of samples in 1.0 M KOH (mF) and C_s is the specific capacitance of the catalyst (C_s = 0.04 mF cm^{-2} in 1.0 M KOH).

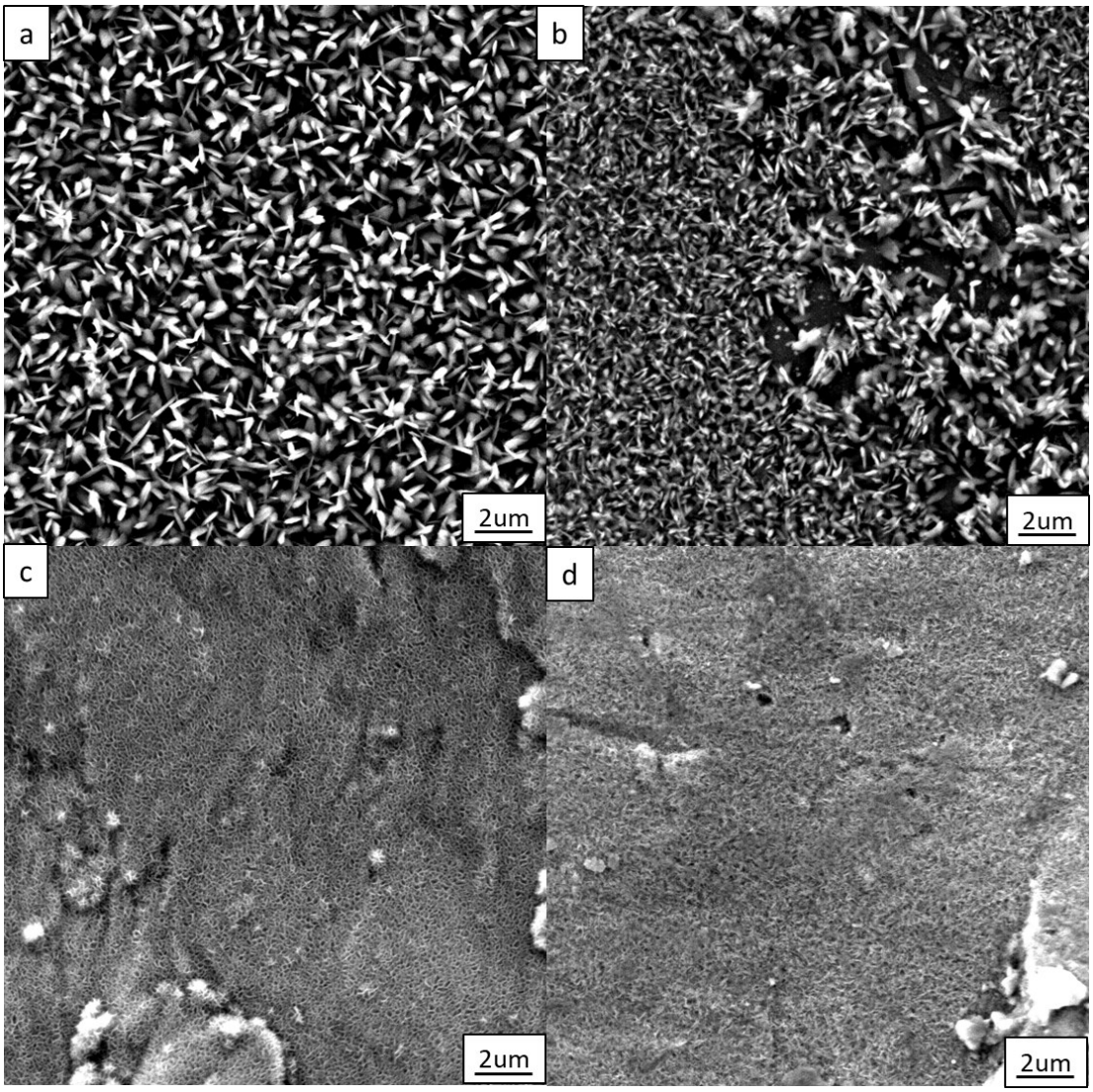

Fig. S11 SEM images after 48h stability test: a) MSG sample, b) FeOOH@MSG sample, c) NG sample and d) FeOOH@NG sample, respectively.

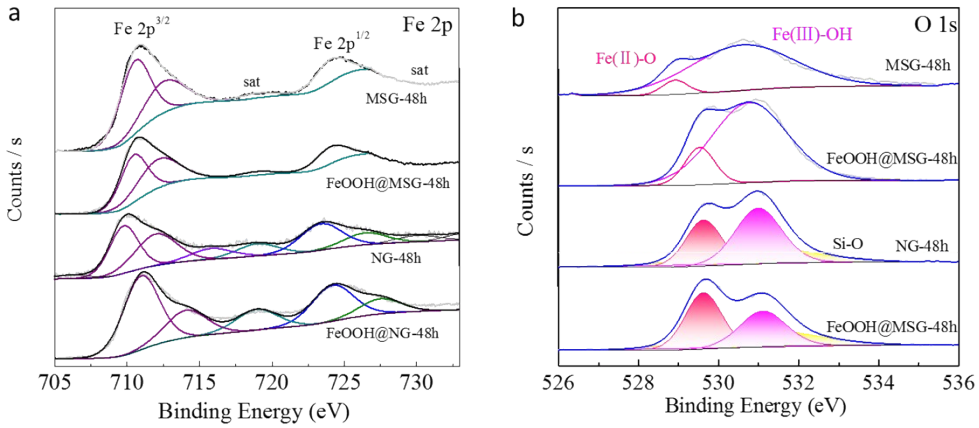

Fig. S12 XPS curves of the all samples after 48h stability test: a) Fe 2p, b) O 1s.

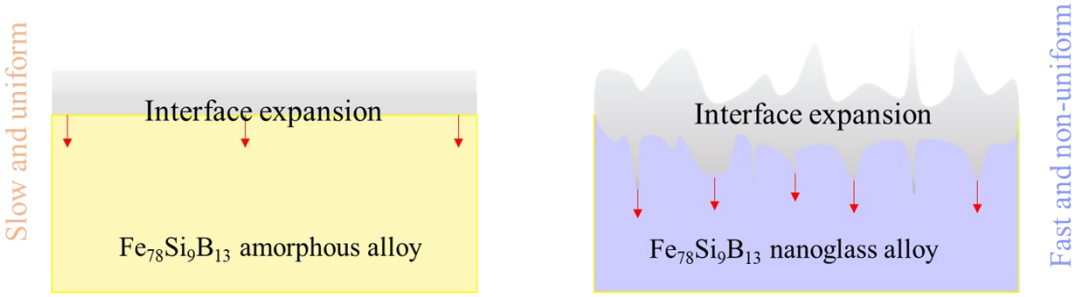

Fig. S13 Schematic diagram of the interface expansion process between $Fe_{78}Si_9B_{13}$ amorphous alloy and Fe-based nanoglass alloy.

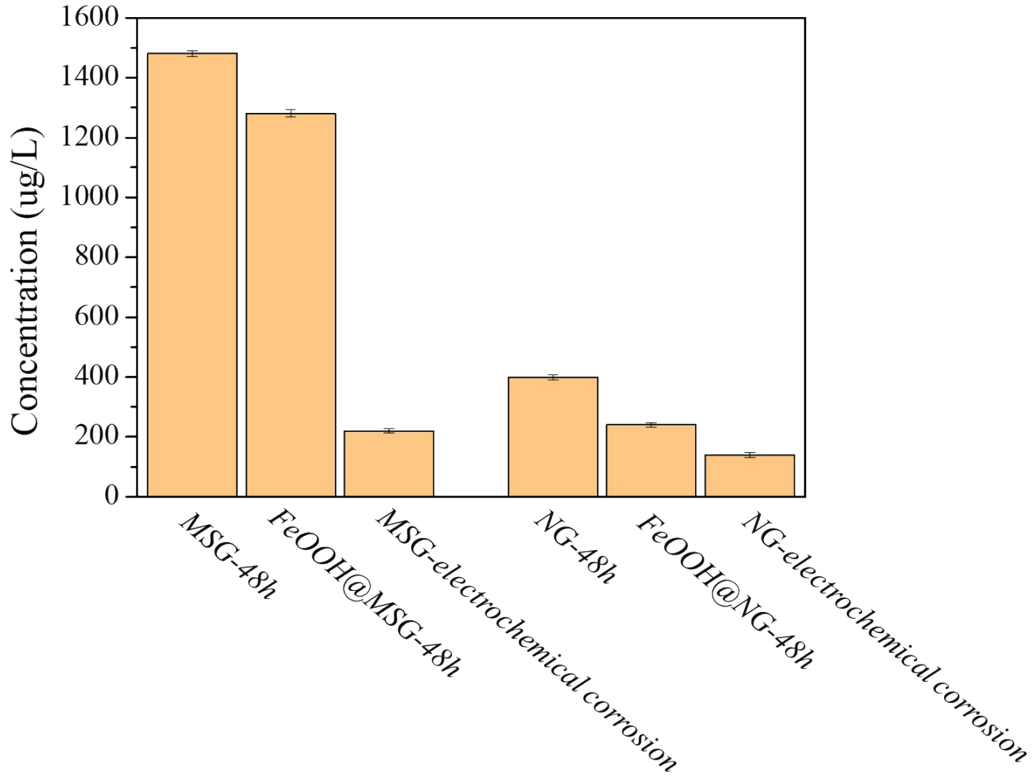

Fig. S14 Histogram of Fe element concentration by ICP-OES.

References

1. Magisetty, R.; Shukla, A.; Kandasubramanian, B., Magnetodielectric Microwave Radiation Absorbent Materials and Their Polymer Composites. *Journal of Electronic Materials* **2018,** *47* (11), 6335-6365.
2. Jia, Z.; Kang, J.; Zhang, W. C.; Wang, W. M.; Yang, C.; Sun, H.; Habibi, D.; Zhang, L. C., Surface aging behaviour of Fe-based amorphous alloys as catalysts during heterogeneous photo Fenton-like process for water treatment. *Applied Catalysis B: Environmental* **2017,** *204*, 537-547.
3. Hedenstedt, K.; Bäckström, J.; Ahlberg, E., In-Situ Raman Spectroscopy of α- and γ-FeOOH during Cathodic Load. *Journal of The Electrochemical Society* **2017,** *164* (9), H621-H627.